Biosensors and Bioelectronics 129 (2019) 189–197

Contents lists available at ScienceDirect

Biosensors and Bioelectronics

journal homepage: www.elsevier.com/locate/bios

Third generation impedimetric sensor employing direct electron transfer type glucose dehydrogenase

Yuka Ito[a,1], Junko Okuda-Shimazaki[b,c,1], Wakako Tsugawa[a], Noya Loew[c], Isao Shitanda[d], Chi-En Lin[e], Jeffrey La Belle[e], Koji Sode[a,b,c,*]

[a] Department of Biotechnology and Life Science, Graduate School of Engineering, Tokyo University of Agriculture and Technology, 2-24-16 Naka-cho, Koganei, Tokyo 184-8588, Japan
[b] Ultizyme International Ltd., 1-13-16, Minami, Meguro, Tokyo 152-0013, Japan
[c] Joint Department of Biomedical Engineering, University of North Carolina at Chapel Hill, Chapel Hill, North Carolina 27599 and North Carolina State University, Raleigh, NC 27695, USA
[d] Department of Pure and Applied Chemistry, Faculty of Science and Technology, Tokyo University of Science, Noda, Chiba 278-8510, Japan
[e] School of Biological and Health System Engineering, Ira A. Fulton Schools of Engineering, Arizona State University, P.O.Box 879709, Tempe, AZ 85287-9719, USA

ARTICLE INFO

Keywords:
Faradaic electrochemical impedance spectroscopy
Impedimetric biosensor
Direct electron transfer
FAD dependent glucose dehydrogenase complex
Charge transfer resistance
Imaginary impedance monitoring

ABSTRACT

Faradaic electrochemical impedance spectroscopy (faradaic EIS) is an attractive measurement principle for biosensors. However, there have been no reports on sensors employing direct electron transfer (DET)-type redox enzymes based on faradaic EIS principle. In this study, we have attempted to construct the 3rd-generation faradaic enzyme EIS sensor, which used DET-type flavin adenine dinucleotide (FAD) dependent glucose dehydrogenase (GDH) complex, to elucidate its characteristic properties as well as to investigate its potential application as the future immunosensor platform. The gold disk electrodes (GDEs) with DET-type FADGDH prepared using self-assembled monolayer (SAM) showed the glucose concentration dependent impedance change, which was confirmed by the change in the charge transfer resistance (R_{ct}). The $\Delta(1/R_{ct})$ values were also affected by DC bias potential and the length of SAM. Based on the Nyquist plot and Bode plot simulations, glucose sensing by imaginary impedance monitoring under fixed frequency (5 mHz) was carried out, revealing the higher sensitivity at low glucose concentration with wider linear range (0.02–0.2 mM). Considering this high sensitivity toward glucose, the 3rd-generation faradaic enzyme EIS sensor would provide alternative platform for future impedimetric immunosensing system, which does not use redox probe.

1. Introduction

Enzyme-based electrochemical biosensors are important in medical care to detect or monitor biomarkers of diseases. The chronoamperometry measurement is one of the most popular methods applied in enzyme sensors. Considering the history of the development of amperometric enzyme sensors, three generations were reported according to their electron acceptors (Ferri et al., 2011). The 1st-generation is based on oxidase. In this principle, oxygen serves as the electron acceptor of the enzyme reaction, and the decreasing oxygen concentration or liberating hydrogen peroxide is detected electrochemically. The 2nd-generation principle uses artificial electron acceptors (mediators) for the enzyme reaction, instead of oxygen, and the reduced artificial electron acceptors are measured electrochemically. The 3rd-generation principle uses enzymes with the ability to transfer electrons directly to the electrodes without the need for oxygen or mediators; these enzymes are called direct electron transfer (DET)-type enzymes.

In addition to the chronoamperometry measurement, faradaic electrochemical impedance spectroscopy (faradaic EIS) has been vigorously studied as the principle of biosensors (Katz and Willner, 2003; Lisdat and Schäfer, 2008). Considering that faradaic EIS is a powerful method to investigate the surface of electrodes in details, variety of faradaic EIS-based immunosensors, which are based on measuring the charge transfer resistance (R_{ct}) of redox probes at the surface of electrodes, have been reported (Afkhami et al., 2017; Attar et al., 2016; Aydin et al., 2019; Aydın et al., 2018; Fusco et al., 2017; Hou et al., 2013, 2014a, 2014b, 2015; Prodromidis, 2010; Ruecha et al., 2019).

* Corresponding author at: Joint Department of Biomedical Engineering, University of North Carolina at Chapel Hill, Chapel Hill, North Carolina 27599 and North Carolina State University, Raleigh, NC 27695, USA.
E-mail address: ksode@email.unc.edu (K. Sode).
[1] These authors contributed equally to this work.

https://doi.org/10.1016/j.bios.2019.01.018
Received 30 June 2018; Received in revised form 12 December 2018; Accepted 2 January 2019
Available online 16 January 2019
0956-5663/

One of the inherent limitations of currently reported faradaic EIS-based immunosensors is the presence of redox probes, which is mandatory to monitor the binding of target molecules to antibodies which alter the flux of redox probes to the electrode surface, consequently, result the change of R_{ct}. However, the redox probes are generally chemically unstable, and the configuration of continuous monitoring and/or *in vivo* monitoring type immunosensors using redox probes are complicated and difficult. Therefore, the development of alternative EIS sensor platforms, which make the robust measurements, have been expected.

It has also been reported about enzyme-based faradaic EIS biosensors; they can be categorized similar to amperometric enzyme sensors. Among the 1st-generation faradaic EIS biosensors, Wang et al. (2015) reported a glucose oxidase-based glucose sensor, which detected the reduction of hydrogen peroxide generated from the glucose oxidase catalytic reaction to measure glucose. Among the 2nd-generation faradaic EIS biosensors, Shervedani et al. (2006) reported a glucose oxidase-based glucose sensor, which detected the oxidation of hydroquinone as a mediator reduced from parabenzoquinone by an enzyme catalytic reaction. However, these faradaic enzyme EIS sensors employed redox mediators or oxygen as the external electron acceptors, therefore, the application of these principle as the alternate platform technology of faradaic EIS-based immunosensors will not solve the above mentioned inherent issue due to the presence of redox probes.

Previously, we reported a flavin adenine dinucleotide (FAD) dependent glucose dehydrogenase (GDH) complex derived from *Burkholderia cepacia*, and its application for biosensor development (Inose et al., 2003; Sode et al., 1996, 2017; Tsuya et al., 2006; Yamaoka and Sode, 2007; Yamaoka et al., 2004; Yamazaki et al., 1999; Yamashita et al., 2013). This FADGDH complex consisted of three subunits: a catalytic subunit which has FAD and 3Fe-4S-type iron-sulfur cluster, an electron transfer subunit which has 3 hemes, and a small subunit as a hitchhiker protein. The electrons generated from oxidation of glucose at FAD in the catalytic subunit are transferred to 3Fe-4S-type iron-sulfur cluster in the catalytic subunit. Then the electrons are transferred to 3rd heme in the electron transfer subunit from 3Fe-4S-type iron-sulfur cluster. Finally, 2nd heme receives the electrons from 3rd heme and transfers the electrons to electrodes directly (Shiota et al., 2016; Yamashita et. al, 2018). Because the electron transfer subunit allows electrons generated from the enzyme catalytic reaction to transfer directly to the electrodes without the need for oxygen or mediators, this FADGDH complex is categorized as DET-type enzyme (DET-type FADGDH). Thanks to the superior characteristic of this DET-type FADGDH, we have reported variety of sensors with DET principles, including DET-type amperometric sensors (Lee et al., 2018; Okuda-Shimazaki et al., 2008; Yamashita et al., 2013, 2018; Yamazaki et al., 2008), biocapacitor type devices (Hanashi et al., 2009, 2011, 2012, 2014; Lee et al., 2017) or potentiometric glucose sensors (Kakehi et al., 2007; Lee et al., 2019), which are proposed to apply for the glucose sensor strips or continuous glucose monitoring. In addition, by creating engineered DET-type GDHs, several attempts to construct DET-type amperometric sensors have been also reported (Algov et al., 2017; Ito et al., 2019; Okuda and Sode, 2004; Okuda et al., 2007; Okuda-Shimazaki et al., 2018). However, there have been no reports on sensors employing DET-type redox enzymes based on faradaic EIS principle.

In this study, we have attempted to construct 3rd-generation faradaic enzyme EIS sensor, which used DET-type FADGDH, to elucidate its characteristic properties as well as to investigate its potential application as the future immunosensor platform. Herein, we modified DET-type FADGDH complex on gold disk electrodes (GDEs) via a self-assembled monolayer (SAM) (Fig. 1). We compared the faradaic enzyme EIS sensors employing either with DET-type FADGDH or with non-DET-type recombinant engineered FADGDH derived from *Aspergillus flavus* (Sakai et al., 2015) in the absence of electron mediators, revealing the sensor with DET-type FADGDH alone showed impedance change depend on glucose concentration. The detail investigation of bias potential and the length of SAM on the impedance dependency were carried out. Based on the Nyquist plot and Bode plot simulations, glucose sensing by fixed frequency based real and imaginary impedance monitoring were carried out. Finally, the characteristics and potential application of 3rd-generation faradaic enzyme EIS sensor for future biosensor platform are discussed.

2. Materials and methods

2.1. Materials

Two types of FADGDH were used. The first was a bacterial DET-type FADGDH complex, which was mutated to improve its substrate specificity and stability (Yamashita et al., 2013). A recombinant DET-type FADGDH complex was prepared using the expression vectors pTrc99A containing the structural gene for the FADGDH complex and pACYC184 containing the structural gene for cytochrome *c* maturation (pEC86). The vectors were transformed into *Escherichia coli* strain BL21 (DE3), cultivated, and recombinant enzyme was prepared as previously described (Tsuya et al., 2006). The other type was fungi-derived FADGDH, which was mutated to improve its stability (Sakai et al., 2015). This FADGDH does not have DET ability to electrodes (herein after as non-DET-type FADGDH). A recombinant non-DET-type FADGDH was prepared using the expression vector pET-30c(+) containing the structural gene for non-DET-type FADGDH. The vectors were transformed into *Escherichia coli* strain Origami2 (DE3) and cultivated as previously described (Sakai et al., 2015).

Dithiobis(succinimidyl hexanoate) (DSH), dithiobis(succinimidyl octanoate) (DSO) and dithiobis(succinimidyl undecanoate) (DSU) were purchased from Dojindo Molecular Technologies, Inc. (Kumamoto, Japan). GDEs and silver/silver chloride (Ag/AgCl) reference electrodes, 1 μm polishing diamond, 0.05 μm polishing alumina, diamond polishing pads, and alumina polishing pads were purchased from BAS Inc. (Tokyo, Japan). Platinum wires were purchased from Tanaka Kikinzoku Kogyo K.K. (Tokyo, Japan). Acetone, H_2O_2, and D(+)-glucose were purchased from Wako Pure Chemical Industries, Ltd. (Osaka, Japan). KOH, $K_3[Fe(CN)_6]$, $NaH_2PO_4{\cdot}2H_2O$, and $Na_2HPO_4{\cdot}12H_2O$ were purchased from Kanto Chemical Co., Inc. (Tokyo, Japan).

2.2. Preparation of DET-type or non-DET-type FADGDH-modified GDEs

GDEs (Electrode surface area: 7 mm^2) were polished using a 1 μm polishing diamond and 0.05 μm polishing alumina on each polishing pad. After GDEs were polished, they were sonicated in distilled water for 15 min. Next, the surfaces of GDEs were cleaned by removing the contamination on the GDEs as follows with reference to the paper of Fiscer et al. (2009). GDEs were soaked in a solution of 50 mM KOH and 25% H_2O_2 for 10 min before rinsing with distilled water. After the treatment, GDEs were placed in 50 mM KOH and connected to a potentiostat. The potential was swept from -200 to −1200 mV vs. Ag/AgCl once, at a 50 mV/s scan rate, and then the GDEs were rinsed with acetone. After cleaning the surfaces of GDEs, the GDEs were incubated in 200 μL of 10 μM DSH, DSO or DSU solution dissolved in acetone overnight at 25 °C to immobilize SAM via covalent conjugation between gold and thiol (Fig. S1). The SAM-modified GDEs were then washed with acetone and incubated in 1 mL of 100 mM phosphate buffer (pH 7.0) including 0.015 mg/mL DET-type FADGDH or non-DET-type FADGDH overnight at room temperature to immobilize the enzyme via covalent conjugation between succinimide of SAM and lysine group of the enzymes (Lee et al., 2018) (Fig. S1). The FADGDH-modified GDEs were stored in 100 mM phosphate buffer (pH 7.0) at 4 °C until use.

2.3. Characterization of GDE surface modification using redox probe

Bare GDEs, SAM-modified GDEs, and DET-type or non-DET-type FADGDH-modified GDEs were evaluated by electrochemical impedance spectroscopy (EIS) to analyse faradaic impedance in 100 mM phosphate

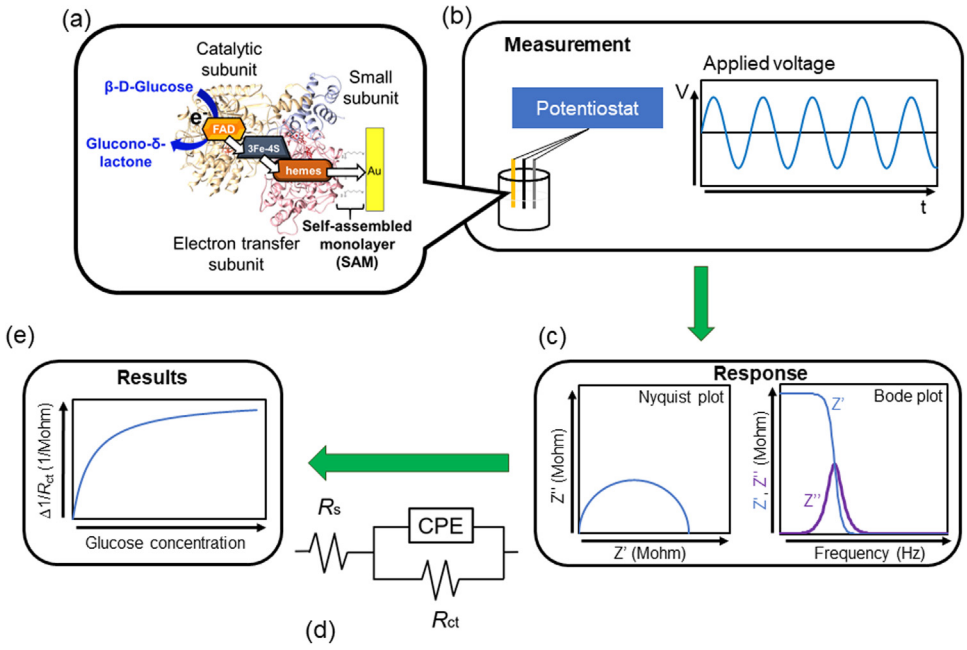

Fig. 1. Schematic diagram of the 3rd-generation faradaic enzyme EIS sensor employing DET-type FADGDH. (a) FADGDH modified GDEs. Bacterial FADGDH, which is capable of DET, was immobilized on GDEs by using SAM. The DET-type FADGDH is composed of three subunits: a catalytic subunit, an electron transfer subunit, and a small subunit. DET-type FADGDH can transfer electrons to the surface of the enzyme structure by intramolecular charge transfer from FAD via 3Fe-4S to multiple hemes. Then, the electrons are transferred from the hemes to the electrodes directly. (b) EIS measurement. FADGDH-modified GDEs were connected to a potentiostat as working electrode. Ag/AgCl and Pt wire were utilized as the reference and counter electrodes. FADGDH modified GDEs were evaluated by EIS. EIS measurement was performed by applying AC voltage superimposed DC potential. (c) Nyquist plots and Bode plots. Imaginary impedance (Z'') obtained from (b) was plotted against real impedance (Z'). Imaginary and real impedance were plotted against Frequency. (d) Equivalent circuit. Description of the equivalent circuit was shown in Section 2.5 and in Fig. 2S. (e) Response curve depending on the substrate of enzyme. Correlation between glucose concentrations and $\Delta(1/R_{ct})$ values obtained by EIS using FADGDH-modified GDEs.

buffer (pH 7.0) containing 10 mM $[Fe(CN)_6]^{3-}$, with Ag/AgCl and Pt wire as the reference and counter electrodes, respectively. EIS measurement was performed in the frequency range 100 kHz-1 Hz by applying AC voltage with an amplitude of 10 mV superimposed on DC potential of + 200 mV vs. Ag/AgCl, using SP-150 (Bio-Logic Science Instruments). Evaluations were carried out in triplicate (N = 3).

2.4. EIS evaluation of DET-type FADGDH and non-DET-type FADGDH-modified GDEs without redox probe

DET-type FADGDH-modified GDEs and non-DET-type FADGDH-modified GDEs were evaluated by EIS to analyse faradaic impedance in 100 mM phosphate buffer (pH 7.0) containing different concentrations of glucose, with Ag/AgCl and Pt wire as the reference and counter electrodes, respectively. EIS measurement was performed in the frequency range 100 kHz-5 mHz by applying AC voltage with an amplitude of 10 mV superimposed on DC potential of + 400, + 100, and −150 mV vs. Ag/AgCl, using SP-150 (Bio-Logic Science Instruments). Evaluations were carried out in triplicate (N = 3).

2.5. Data analysis

Generally, the obtained EIS data were analysed with an equivalent circuit to obtain electrochemical parameters. In this study, Randles equivalent circuit without the Warburg impedance (W), including the resistance of the electrolyte solution (R_s), the constant phase element (CPE), and the charge transfer resistance (R_{ct}) was used (Supplementary information Fig. S2). At this time the double layer capacitance was replaced by CPE. In general, the value of real impedance (Z') of the initial plots of the Nyquist diagrams indicates the resistance of the electrolyte solution (R_s), if the situation of EIS measurement can be expressed as the equivalent circuit in Fig. S2. After performing EIS, the R_{ct} values were calculated by fitting the Nyquist plots by using ZView (Scribner Associates, Inc. Version 3.5c).

2.6. Simulation

Nyquist plot and Bode plot of each glucose concentrations including the range of low frequencies were simulated by calculation of real impedance (Z') and imaginary impedance (Z") using Microsoft Excel. Randles equivalent circuit without the Warburg impedance (W) was used for the simulation as the equivalent circuit of the system (Supplementary information Fig. S2). In the equivalent circuit, real impedance (Z') and imaginary impedance (Z") can be calculated using the equations as follows (Vadim, 2012).

$$Z' = R_s + \frac{R_{ct}}{1+\omega^2 {R_{ct}}^2 {C_{dl}}^2} \quad (1)$$

$$Z' = \frac{\omega {R_{ct}}^2 C_{dl}}{1+\omega^2 {R_{ct}}^2 {C_{dl}}^2} \quad (2)$$

ω, which is angular frequency, was calculated by frequency in the range of 100 kHz-1 μHz. R_s, R_{ct} and C_{dl} were obtained by experimental EIS measurements (Section 2.5).

2.7. Glucose detection using of 3rd-generation faradaic enzyme EIS sensor with fixed frequency measurements

DET-type FADGDH-modified GDE was evaluated by EIS in 100 mM phosphate buffer (pH 7.0) containing low concentrations of glucose (f.c. 0.02, 0.03, 0.05, 0.1, 0.2 mM), with Ag/AgCl and Pt wire as the reference and counter electrodes, respectively. EIS measurement was performed at the frequency of 5 mHz by applying AC voltage with an amplitude of 10 mV superimposed on DC potential of + 100 mV vs. Ag/AgCl, using SP-150 (Bio-Logic Science Instruments). Evaluations were carried out in triplicate (N = 3).

3. Results

3.1. Characterization of GDE surface modification using redox probe

EIS with redox probes is a powerful method for investigating the

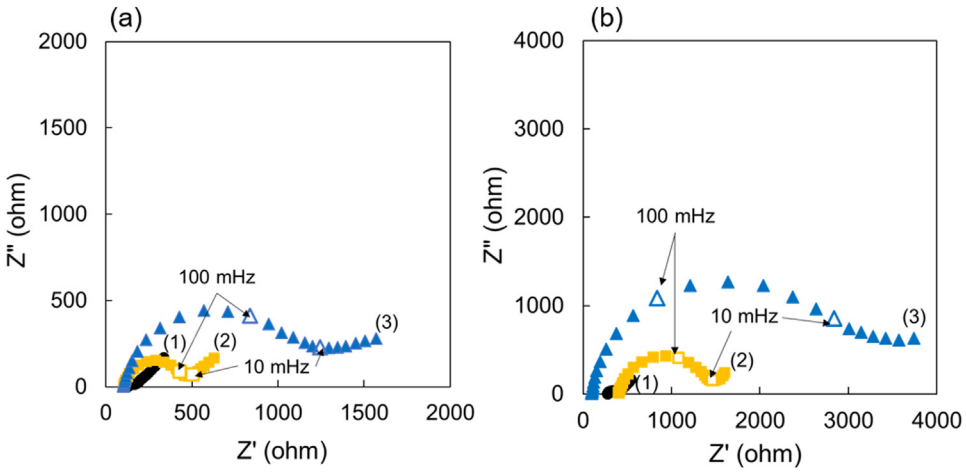

Fig. 2. EIS was performed in 100 mM phosphate buffer (pH 7.0) containing 10 mM $[Fe(CN)_6]^{3-}$ using GDEs at each modification step of (a) DET-type FADGDH-modified GDEs and (b) non-DET-type FADGDH-modified GDEs. EIS measurement was performed in the frequency range 100 kHz-1 Hz by applying AC voltage with an amplitude of 10 mV superimposed on DC potential of + 200 mV vs. Ag/AgCl. (1) Black circles, (2) yellow squares, and (3) blue triangles show Nyquist plots of bare GDEs, GDE/DSH, and GDE/DSH/FADGDH, respectively. Evaluations were carried out in triplicate (N = 3) and Fig. 2 shows representative data.

surface condition of the electrodes by monitoring the electron flux of the redox probes. To evaluate the surface modification process of the GDEs, EIS was performed on the GDEs from each modification step with $[Fe(CN)_6]^{3-}$ as the redox probe at + 200 mV vs. Ag/AgCl, which is around the midpoint of $[Fe(CN)_6]^{3-}$. At this potential, we can ignore the effect of the small amount of $[Fe(CN)_6]^{4-}$ converted from $[Fe(CN)_6]^{3-}$, because the effect of $[Fe(CN)_6]^{4-}$ should be cancelled among bare electrodes, SAM-modified electrodes and enzyme-modified electrodes by comparing the R_{ct} values among them. Fig. 2 shows the Nyquist plots, indicating each modification process of the DET-type FADGDH or non-DET-type FADGDH-modified GDEs using DSH. Comparing the modified GDEs with the bare GDEs, the diameter of semi-circles, which indicate R_{ct} values, became larger when the modified GDEs were evaluated by EIS. By fitting the Nyquist plots with the equivalent circuit (Fig. S2), the values of R_{ct} were estimated to be 69.89, 473.4, and 1328 Ω for the bare GDE, GDE/DSH, and GDE/DSH/DET-type FADGDH, respectively, and 153.2, 1157, and 3417 Ω for the bare GDE, GDE/DSH, and GDE/DSH/non-DET-type FADGDH, respectively. After DSH was modified on the GDEs surface, the R_{ct} values increased. Moreover, after FADGDH was modified on the DSH-modified GDEs, the R_{ct} values further increased. The R_{ct} value is a useful parameter for investigating the surface phenomena, because the R_{ct} value is affected by the energy barrier of the redox probes reaching the electrodes. In this case, it became difficult for $[Fe(CN)_6]^{3-}$ as redox probes to access the surface of the modified GDEs. Cyclic voltammetry measurement was also performed using bare GDEs, SAM-modified GDEs, and DET-type or non-DET-type FADGDH-modified GDEs in the presence of $[Fe(CN)_6]^{3-}$ as redox probes (Supplementary information Fig. S3). As shown in Fig. S3, oxidation and reduction peak current of SAM and the enzymes-modified GDEs became decreased, comparing the modified GDEs with the bare GDEs. This result indicates the accessibility of $[Fe(CN)_6]^{3-}$ to electrodes decreased due to steric hinderance of SAM and SAM with the enzymes. Therefore, it was confirmed that SAM- and DET-type FADGDH and non-DET-type FADGDH-modified GDEs were constructed.

3.2. Glucose measurement by 3rd-generation faradaic enzyme EIS sensor without mediators

The impedimetric analyses of DET-type FADGDH and non-DET-type FADGDH-modified GDEs responses toward glucose were carried out in the absence of mediators. Fig. 3(a) shows the Nyquist plots for different concentrations of glucose using GDE/DSH/DET-type FADGDH obtained in a pH 7.0 phosphate buffer with a frequency range 100 kHz–5 mHz at an amplitude of 10 mV superimposed on DC potential of + 100 mV vs. Ag/AgCl. (Bode plots of EIS measurement using DET-type FADGDH-modified GDE are shown in Supplementary Information, Fig. S4) In general, diameter of Nyquist plot drawing a semi-circle indicates the R_{ct} value when the electrochemical reactions on the electrodes can be expressed the equivalent circuit as shown in Fig. S2. At this time, precise numbers for R_{ct} were obtained by fitting the Nyquist plots of GDE/DSH/DET-type FADGDH using the equivalent circuit (Supplementary Information Fig. S2). When EIS was performed without glucose, an adequate semi-circle on the Nyquist plot was not obtained. The reason why an adequate semi-circle on the Nyquist plot was not obtained when EIS was performed without glucose is the R_{ct} values got too large (R_{ct} > 40 Mohm). On the contrary, when EIS was performed in the presence of glucose, semi-circles on the Nyquist plots were observed. Furthermore, the obtained semi-circles on the Nyquist plots became smaller with increasing glucose concentrations at glucose concentration range 1–100 mM. In addition, the result that the obtained semi-circles on the Nyquist plots got smaller upon increasing glucose concentrations indicates that the R_{ct} values decreased depending on glucose concentrations, reaching R_{ct} = 3.8 Mohm at 100 mM of glucose.

To demonstrate that impedance obtained by EIS is changed depending on DET, the non-DET-type FADGDH-modified GDEs were evaluated in the same manner as the DET-type FADGDH-modified GDEs. As shown in Fig. 3(b), impedance was not changed, showing identical Nyquist plots in the glucose concentrations range from 0 to 100 mM. Furthermore, adequate semi-circles could not be obtained at each glucose concentration. The electrons generated from the catalytic reaction of non-DET-type FADGDH are expected not to be transferred without adding redox mediators so that the obtained impedance was not be changed with increasing glucose concentrations.

These results indicated that the observed glucose concentration dependent impedance change with DET-type FADGDH-modified GDE was confirmed by the DET reaction, which changes the R_{ct} values.

Fig. 3(c) shows the correlation between Δ ($1/R_{ct}$) values and glucose concentrations. Δ ($1/R_{ct}$) is defined as follows.

$$\Delta(1/R_{ct}[\text{glucose conc}]) = 1/R_{ct}\ \ [\text{glucose conc}] - 1/R_{ct}[0\ \text{mM}]$$

As shown in Fig. 3(c), the$\Delta(1/R_{ct})$ values increased with the increase of glucose concentrations. The linearity range was 0–10 mM glucose. The corresponding function within the range was $y(1/\text{ohm}) = 1.3\times10^{-8}x\ \ (\text{mM})+2.5\times10^{-8}$.

Therefore, by making a comparison between the results of DET-type FADGDH and non-DET-type FADGDH, EIS with DET-type FADGDH-modified GDEs showed impedance depend on glucose concentration, the 3rd-generation faradaic EIS biosensor was constructed.

We also investigated the stability under the continuous operation of 3rd-generation faradaic enzyme EIS sensor by repeating EIS measurement to prepare Nyquist plots, continuously for 191 times (171 h) with 20 mM glucose. As the results, with the repeating measurements, the R_{ct} values gradually increased, consequently $1/R_{ct}$ value decreased, which

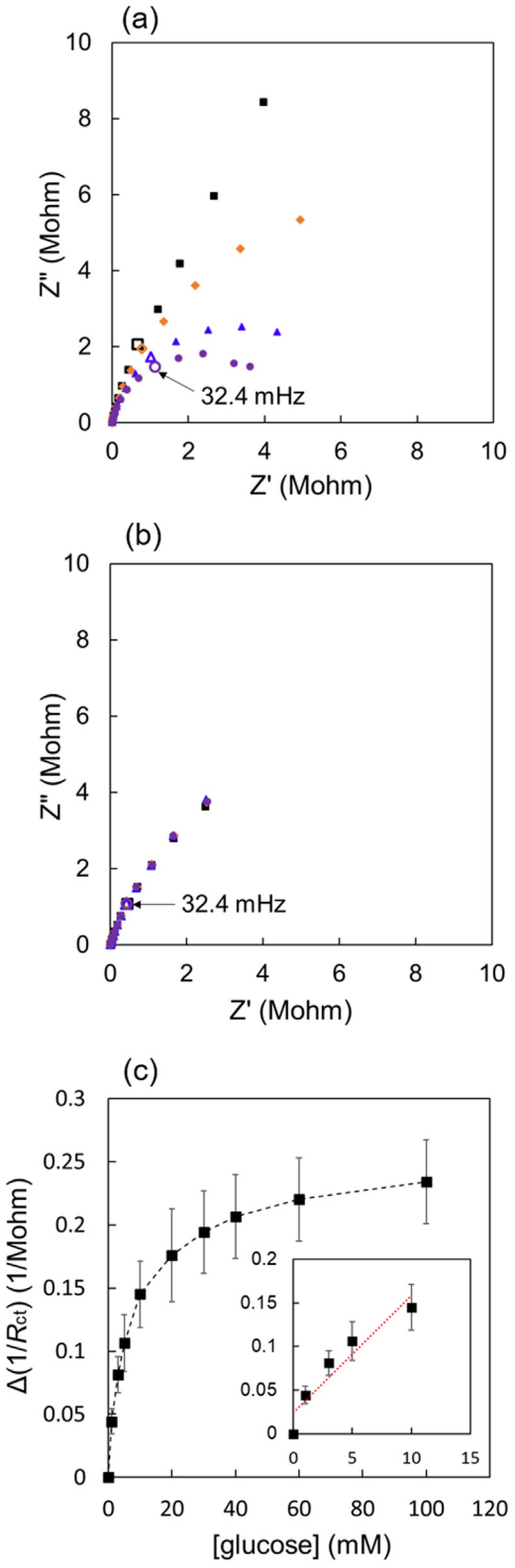

Fig. 3. EIS analyses with DET-type FADGDH-modified GDEs or non-DET-type FADGDH-modified GDEs. EIS was performed in 100 mM phosphate buffer (pH 7.0) containing glucose using (a) DET-type FADGDH-modified GDEs or (b) non-DET-type FADGDH-modified GDEs. EIS measurement was performed in the frequency range 100 kHz-5 mHz by applying AC voltage with an amplitude of 10 mV superimposed on DC potential of + 100 mV vs. Ag/AgCl. Black squares, orange diamonds, blue triangles and purple circles show Nyquist plots at glucose concentrations of 0, 1, 10, and 100 mM, respectively. Evaluations were carried out in triplicate (N = 3). (c) Correlation between glucose concentrations and $\Delta(1/R_{ct})$ values obtained by EIS using GDE/DSH/DET-type FADGDH. DET-type FADGDH-modified GDEs applying AC voltage with an amplitude of 10 mV superimposed on DC potential of + 100 mV vs. Ag/AgCl in the frequency range 100 kHz–5 mHz. The function of the calibration curve within the range of 0–10 mM glucose was $y(1/ohm) = 1.3\times10^{-8}x$ (mM)$+2.5\times10^{-8}$ (R^2 = 0.894). Evaluations were carried out in triplicate (N = 3).

we used as the readout for the glucose concentration in Fig. 3(c). After the 191 measurement, the readout decreased to 32% of the initial value. In our previous study, using same electrode configuration, continuous amperometric operation of this electrode was reported (Lee et al., 2018), where no significant decrease was observed after 20 h continuous operation. Besides, under the continuous EIS measurement in this study, about 83% of the initial readout of $1/R_{ct}$ value was observed. Therefore, the stability of the electrode would be slightly lower compared with the operation under amperometric measurement. (Supplementary information, Fig. S5).

3.3. Parameter analysis influencing to R_{ct}

We investigated the parameters affect R_{ct} values. We focused on the DC bias potential and the length of the SAM because these parameters must affect the efficiency of DET.

Fig. 4(a) shows the $\Delta(1/R_{ct})$ values at each glucose concentration obtained by EIS without mediators performed on GDE/DSH/DET-type FADGDH at DC bias potential of + 400, + 100, and −150 mV vs. Ag/AgCl. The $\Delta(1/R_{ct})$ values were extremely low at the applied potential of −150 mV vs. Ag/AgCl. Moreover, there is no correlation between glucose concentrations and the $\Delta(1/R_{ct})$ values at −150 mV vs. Ag/AgCl. On the contrary, when EIS was performed at the applied potential of + 400 or + 100 mV vs. Ag/AgCl, the $\Delta(1/R_{ct})$ values were much higher. In addition, the $\Delta(1/R_{ct})$ values of + 400 or + 100 mV vs. Ag/AgCl increased with the increase of glucose concentrations. Thus, it is confirmed that DET causes the change of the $\Delta(1/R_{ct})$ values, and the $\Delta(1/R_{ct})$ values are affected by DC bias potential.

Fig. 4(b) shows the $\Delta(1/R_{ct})$ values at each glucose concentrations obtained by EIS for DET-type FADGDH-modified GDEs, which used three types of SAM regents: DSH, DSO and DSU. DSU has a longest carbon chain (14.9–15.4 Å) than DSH (8.3–8.8 Å) and DSO (10.9–11.4 Å). The $\Delta(1/R_{ct})$ values of each GDE/DSH/DET-type FADGDH, GDE/DSO/DET-type FADGDH or GDE/DSU/DET-type FADGDH increased with increasing of glucose concentrations, however the $\Delta(1/R_{ct})$ values were much lower when the DET-type FADGDH was immobilized by DSU, which has a longer carbon chain. The distance between DET-type FADGDH and the electrodes was determined by the length of SAM. We previously reported the strength of DET is affected by the distance between the surface of electrodes and the enzyme (Lee et al., 2018). Therefore, we concluded that the $\Delta(1/R_{ct})$ values are affected by the length of SAM because the length of SAM changes the strength of DET.

3.4. High-sensitive glucose detection using of 3rd-generation faradaic enzyme EIS sensor under fixed frequency measurements

The Nyquist plots and Bode plots were simulated to predict the glucose concentration and frequency dependent change in real and imaginary impedance, including the lower frequencies which were not experimentally investigated (Fig. 5(a), (b), (c)). These simulated results clearly indicated that $1/R_{ct}$, real impedance and imaginary impedance show glucose concentration dependency. All simulation indicates that the impedance changes at lower glucose concentration result larger difference, indicating that 3rd-generation faradaic enzyme EIS provide highly sensitive glucose detection at a lower concentration. Another remarkable feature is that the frequency dependencies of real and

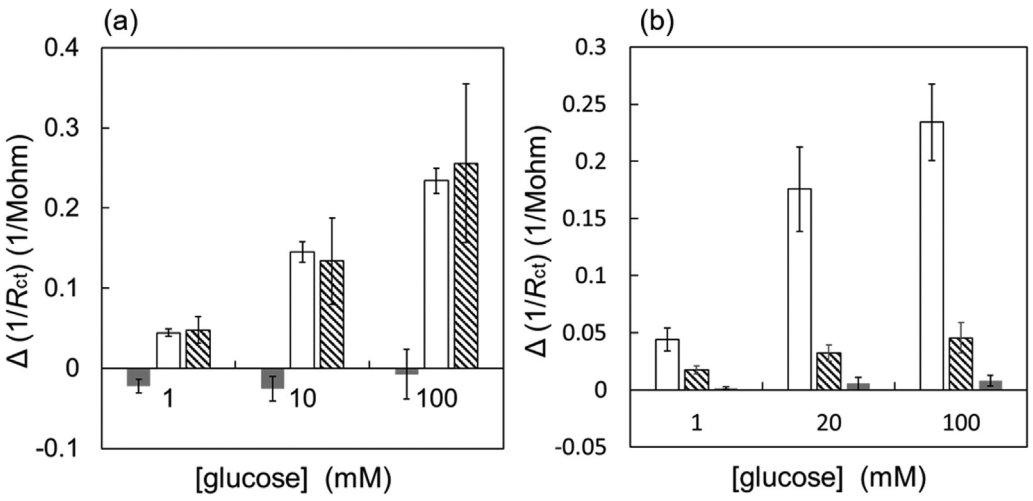

Fig. 4. $\Delta(1/R_{ct})$ values at various glucose concentration. (a) R_{ct} values were obtained by EIS, which was performed in 100 mM phosphate buffer (pH 7.0) using GDE/DSH/DET-type FADGDH at different DC bias potentials; grey, white and angled stripe show -150, + 100, and + 400 mV vs. Ag/AgCl, respectively (frequency range: 100 kHz–5 mHz, amplitude: 10 mV). (b) R_{ct} values were obtained by EIS, which was performed in 100 mM phosphate buffer (pH 7.0) using GDE/DSH/DET-type FADGDH (white), GDE/DSO/DET-type FADGDH (angled stripe) or GDE/DSU/DET-type FADGDH (grey) (DC bias potential: +100 mV vs. Ag/AgCl, frequency range: 100 kHz–5 mHz, amplitude: 10 mV). Evaluations were carried out in triplicate (N = 3).

imaginary impedances are different. It is obvious that the glucose concentration dependency of real impedance is observable at frequencies lower than 2.5 mHz, whereas those of imaginary impedance is observable at much higher frequencies, lower than 15 mHz. These observations suggested that glucose measurement will be possible by monitoring imaginary impedance at a fixed frequency at higher frequency than those for those to monitor real impedance (Fig. 5(b), (c)). Considering that the 3rd-generation faradaic enzyme EIS sensor showed much higher impedance change at lower glucose concentration, and the measurement of $1/R_{ct}$ values, which has been conventionally used as the measure in enzyme-based impedimetric analyses takes a long period of measurement and complicated, the investigation of fixed frequency based impedimetric analyses at lower glucose concentration of this system should be carried out.

Fig. 6 shows the glucose concentration dependencies of real impedance (Fig. 6(a)) and imaginary impedance (Fig. 6(b)) at 5 mHz, respectively. The investigated glucose range was 0.02–0.2 mM range with 0.01 mM resolution at minimum, which was 100 times lower concentration and 200 times higher resolution than those shown in Fig. 3(c) (concentration range; 1–100 mM. minimum resolution; 2 mM). The real impedance showed linear correlation with glucose concentration range between 0.02 mM and 0.05 mM, however, at further higher glucose concentration, constant real impedance was observed. In contrary, as was expected from the results of Bode plot simulation, imaginary impedance showed higher sensitivity at this low glucose range with wider linear range. Good linear correlations (R^2 = 0.996) were observed within the glucose range here investigated (0.02–0.2 mM). These results indicated that imaginary impedance obtained from the fixed frequency (5 mHz) provides highly sensitive glucose concentration measurement with high resolution.

4. Discussion

In this study, we have attempted to construct 3rd-generation faradaic enzyme EIS sensor, which used DET-type FADGDH, to elucidate its characteristic properties as well as to investigate its potential application as the future immunosensor platform. We first investigated the correlation between DET and impedance obtained by EIS from 3 different viewpoints: comparison between DET-type FADGDH and non-DET-type FADGDH, different DC bias potential and the length of SAM. At first, we confirmed obvious difference between DET-type FADGDH and non-DET-type FADGDH to demonstrate DET causes the change of impedance obtained by EIS without redox mediators. Furthermore, glucose dependence of the $\Delta(1/R_{ct})$ values is conformed.

As shown in Fig. 3(c), the $\Delta(1/R_{ct})$ values increased with the increase of glucose concentrations. $1/R_{ct}$ can be expressed as under equilibrium.

$$1/R_{ct} = dI/dE \ (I\text{: current}, E\text{: potential})$$

The equilibrium indicates that the $1/R_{ct}$ values can be changed depending on current when potential is constant. When chronoamperometry measurement was performed in a pH 7.0 phosphate buffer containing various concentrations of glucose at a DC bias potential of + 100 mV vs. Ag/AgCl using GDE/DSH/DET-type FADGDH, the response current increased upon increasing glucose concentrations (Fig. S6). The result shows that the number of electrons which were directly transferred from DET-type FADGDH to the GDEs increased with the increase of glucose concentrations. Therefore, it is confirmed that the $\Delta(1/R_{ct})$ values were related to DET between DET-type FADGDH and the electrodes.

Next, EIS was performed on DET-type FADGDH-modified GDEs at various potential in order to investigate how the efficiency of DET affects the $\Delta(1/R_{ct})$ values. The result suggests that changing efficiency of DET caused by the variation of DC bias potential affects the $\Delta(1/R_{ct})$ values. It was also confirmed that DET occurred at the applied potential of + 400 or + 100 mV vs. Ag/AgCl by performing chronoamperometry measurement, however the response current was extremely low at the applied potential of −150 mV vs. Ag/AgCl (Fig. S7). Moreover, it is demonstrated that the $\Delta(1/R_{ct})$ values are related to the strength of DET by changing the length of SAM.

Therefore, in this study we demonstrated that the R_{ct} value is related to the direct electron transfer (DET) by the enzyme catalytic reaction of the DET-type FADGDH which is affected by three factors; (1) glucose concentration, (2) the length of SAM and (3) DC bias potential.

Vidakovi´c-Koch et al. (2013) previously reported the application of electrochemical impedance spectroscopy for studying the mechanism of an enzymatic process by making a comparison between a theoretical simulation and experimental data. As a model system, horseradish peroxidase (HRP) absorbed on graphite, which shows DET, was chosen (Vidakovi´c-Koch et al., 2013). In contrast, in our study, we experimentally demonstrated form various viewpoints, for the first time, that there was an interrelation between DET and impedance obtained by EIS without redox mediators. Moreover, we investigated the correlation between R_{ct} and DET.

In addition to the measurement of R_{ct} value and its glucose concentration dependency, the glucose concentration dependency of imaginary impedance was observed under fixed frequency (Fig. 6(b)). Although the R_{ct} value measurement provided variety of surface information, however, the period required for the experiments to obtain a single Nyquist plot for one glucose concentration is about 10 min (by

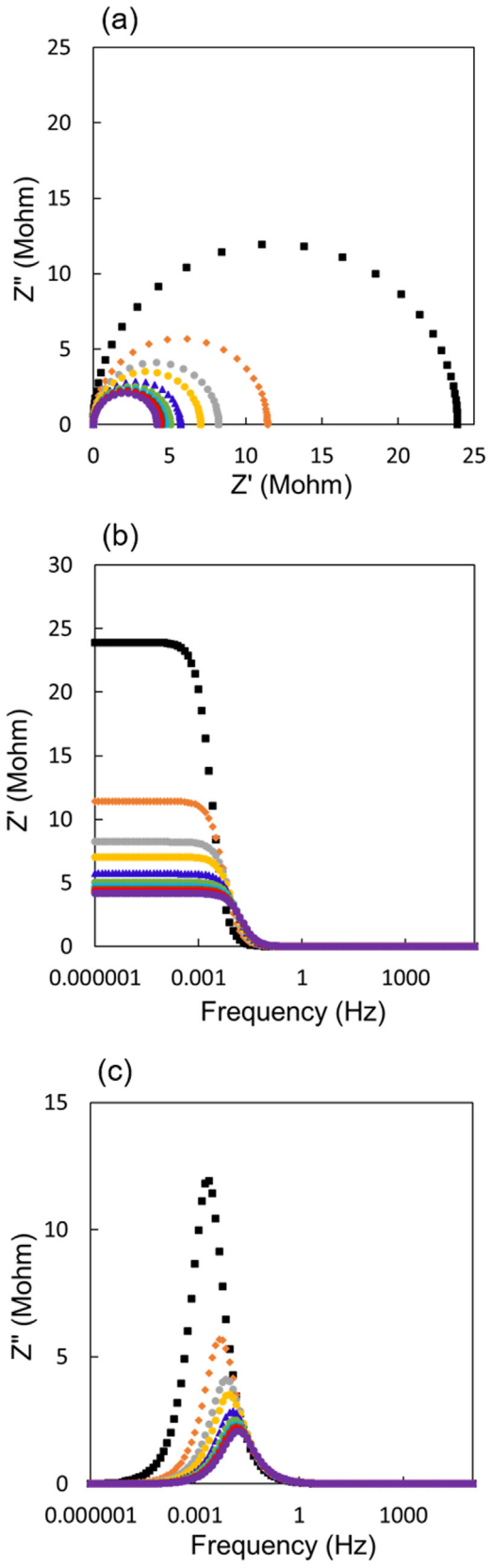

Fig. 5. Simulated Nyquist plots and Bode plots. (a) Nyquist plots of various glucose concentrations (0–100 mM) were simulated including the range of low frequencies (100 kHz-1 μHz). Bode plots of various glucose concentrations (0–100 mM) showing (b) real impedance (Z') and (c) imaginary impedance (Z'') at each frequency were also simulated including the range of low frequencies (100 kHz to 1 μHz). Black squares, orange diamonds, grey circles, yellow circles, blue triangles, green circles, light blue circles, brown circles, red circles and purple circles show simulated Bode plots at glucose concentrations of 0, 1, 3, 5, 10, 20, 30, 40, 60 and 100 mM, respectively.

employing 100 kHz – 5 mHz). To obtain a calibration the correlation between $\Delta(1/R_{ct})$ and glucose concentration, it takes more than 1.6 h to analyse entire glucose concentration range by varying various frequency investigated in this study (10 plots). Moreover, when a single Nyquist plot of lower glucose concentration is obtained to gain the R_{ct} value, it takes much longer hours to obtain a semi-circle of the Nyquist plot including in the range of much lower frequencies. Instead, the Bode plot simulation suggested that glucose concentration dependence of imaginary impedance change will be observable at fixed frequency lower than 15 mHz. By choosing 5 mHz, which took 3 min for single impedance measurement for one glucose concentration, it takes 30 min to obtain the correlation between Δ Z'' and glucose concentration (10 plots). Therefore, these results strongly support that constant frequency based imaginary impedance measurement would be the standard method for 3rd-generation faradaic enzyme EIS sensor. In addition, this investigation showed that 3rd-generation faradaic enzyme EIS sensor provides highly sensitive glucose measurement, compared with those reported in the 1st (Wang et al., 2015) and 2nd (Shervedani et al., 2006) generation type enzyme EIS sensors, which reported glucose range higher than 1 mM with several mM range in the resolution. Considering this high sensitivity toward glucose, the 3rd-generation faradaic enzyme EIS sensor would be applied for the alternative platform for impedimetric immunosensing system, which does not utilize redox probes. Currently reported impedimetric immunosensors employed redox probes to monitor their flux change by the binding of target molecule to the antibodies immobilized on the surface of electrode. The mandatory presence of redox probes limits the potential application of faradaic EIS immunosensors. The method introduced in this study, would provide a novel platform of immunosensor which does not use redox probes, instead glucose flux could be the indicator for the binding of the target to the ligand on the surface of electrode, which might be co-immobilized together with DET type GDH.

Although further investigations are required, our success in revealing that 3rd-generation faradaic enzyme EIS sensor showed glucose dependent impedance change with high sensitivity in the absence of redox probes, would suggest the future development of novel immunosensing system based on the current study.

5. Conclusion

In this study, we have demonstrated, for the first time, the 3rd-generation impedimetric biosensors by performing EIS without redox mediators for DET-type FADGDH-modified GDEs.

When EIS was performed with DET-type FADGDH-modified GDE in the presence of glucose, semi-circles on the Nyquist plots were observed. Furthermore, the obtained semi-circles on the Nyquist plots became smaller with increasing depending on glucose concentrations at glucose concentration range 1–100 mM. On the contrary, EIS analyses of the non-DET-type FADGDH-modified GDEs revealed that no impedance change was observed by changing glucose concentration, showing identical Nyquist plots in the glucose concentrations range from 0 to 100 mM. These results indicated that the observed glucose concentration dependent impedance change with DET-type FADGDH-modified GDE was confirmed by the DET reaction, which changes the R_{ct} values. In addition, the DET-type FADGDH-modified GDEs showed impedance depend on glucose concentration. It was also confirmed that the $\Delta(1/R_{ct})$ values are affected by DC bias potential and also affected by the length of SAM. Based on the Nyquist plot and Bode plot simulations, glucose sensing by imaginary impedance under fixed frequency

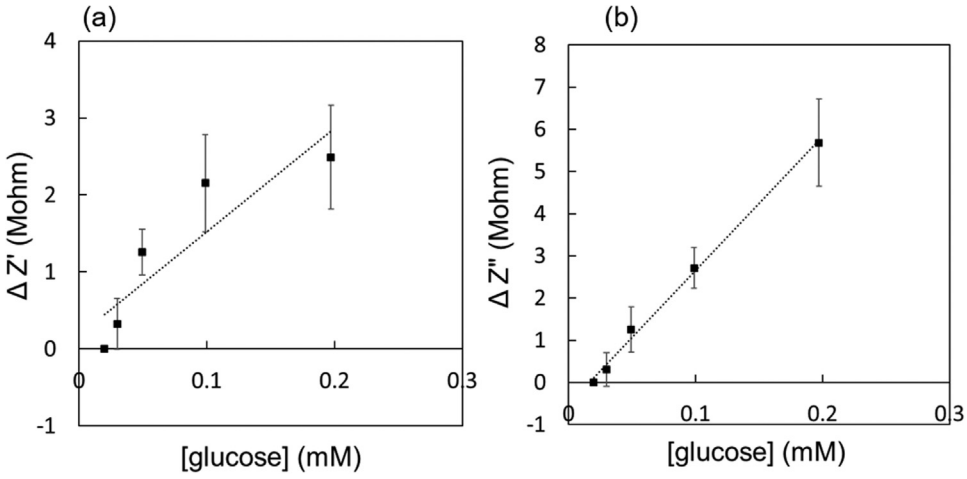

Fig. 6. Correlation between glucose concentrations in the range of 0.02–0.2 mM and (a) real impedance, (b) imaginary impedance. Δ Z' or Δ Z'' indicates the real impedance or imaginary impedance of each glucose concentrations excluded the real impedance or imaginary impedance of 0.02 mM glucose. EIS measurement was performed at the frequency of 5 mHz by applying AC voltage with an amplitude of 10 mV superimposed on DC potential of + 100 mV vs. Ag/AgCl. Evaluations were carried out in triplicate (N = 3) except for (a) real impedance plots of 0.03 mM glucose which shows N = 2 data in order to remove an outlying value. The function of the calibration curve of glucose vs. real impedance within the range of 0.02–0.2 mM glucose was $y(1/ohm) = 1.3\times10^{7}x$ (mM)$+1.8\times10^{5}$ (R^2 = 0.797). The function of the calibration curve of glucose vs. imaginary impedance within the range of 0.02–0.2 mM glucose was $y(1/ohm) = 3.1\times10^{7}x$ (mM)$+5.2\times10^{5}$ (R^2 = 0.996).

(5 mHz) was carried out, revealing the higher sensitivity at low glucose concentration with wider linear range (0.02–0.2 mM). Considering this high sensitivity toward glucose, the 3rd-generation faradaic enzyme EIS sensor would provide alternative platform for future impedimetric immunosensing system, which does not use redox probes.

Acknowledgements

Y. I. was supported by the Japan Student Services Organisation (JASSO) Student Exchange Support Program (Scholarship for Short-term study abroad, FY2016) to research at Arizona State University.

Appendix A. Supporting information

Supplementary data associated with this article can be found in the online version at doi:10.1016/j.bios.2019.01.018.

References

Afkhami, A., Hashemi, P., Bagheri, H., Salimian, J., Ahmadi, A., Madrakian, T., 2017. Impedimetric immunosensor for the label-free and direct detection of botulinum neurotoxin serotype A using Au nanoparticles/graphene-chitosan composite. Biosens. Bioelectron. 93, 124–131.

Algov, I., Grushka, J., Zarivach, R., Alfonta, L., 2017. Highly efficient flavin-adenine dinucleotide glucose dehydrogenase fused to a minimal cytochrome C domain. J. Am. Chem. Soc. 139, 17217–17220.

Attar, A., Mandli, J., Ennaji, M., M., Amine, A., 2016. Label-free electrochemical impedance detection of Rotavirus based on immobilized antibodies on gold sononanoparticles. Electroanalysis 28, 1839–1846.

Aydin, M., Aydin, E., B., Sezgintürk, M., K., 2019. Electrochemical immunosensor for CDH22 biomarker based onbenzaldehyde substituted poly(phosphazene) modified disposable ITOelectrode A new fabrication strategy for biosensors. Biosens. Bioelectron. 126, 230–239.

Aydın, M., Aydın, E., B., Sezgintürk, M., K., 2018. A disposable immunosensor using ITO based electrode modified by a star-shaped polymer for analysis of tumor suppressor protein p53 in human serum. Biosens. Bioelectron. 107, 1–9.

Ferri, S., Kojima, K., Sode, K., 2011. Review of glucose oxidases and glucose dehydrogenases: a bird's eye view of glucose sensing enzymes. J. Diabetes Sci. Technol. 5 (5), 1068–1076.

Fiscer, L., M., Tenje, M., Heiskanen, A., R., Masuda, N., Castillo, J., Bentien, A., Émneus, J., Jakobsen, M., H., Boisen, A., 2009. Gold cleaning methods for electrochemical detection applications. Microelectron. Eng. 86, 1282–1285.

Fusco, G., Gallo, F., Tortolini, C., Bollella, P., Ietto, F., Mico, A., D., D'Annibale, A., Antiochia, R., Favero, G., Mazzei, F., 2017. AuNPs-functionalized PANABA-MWCNTs nanocomposite-based impedimetric immunosensor for 2,4-dichlorophenoxy acetic acid detection. Biosens. Bioelectron. 93, 52–56.

Hanashi, T., Yamazaki, T., Tsugawa, W., Ferri, S., Nakayama, D., Tomiyama, M., Ikebukuro, K., Sode, K., 2009. BioCapacitor—a novel category of biosensor. Biosens. Bioelectron. 24, 1837–1842.

Hanashi, T., Yamazaki, T., Tsugawa, W., Ikebukuro, K., Sode, K., 2011. BioRadioTransmitter: a self-powered wireless glucose-sensing system. J. Diabetes Sci. Technol. 5, 1030–1035.

Hanashi, T., Yamazaki, T., Tsugawa, W., Ikebukuro, K., Sode, K., 2012. BioLC-Oscillator: a self-powered wireless glucose-sensing system with the Glucose dependent resonance frequency. Electrochemistry 80, 367–370.

Hanashi, T., Yamazaki, T., Tanaka, H., Ikebukuro, K., Tsugawa, W., Sode, K., 2014. The development of an autonomous self-powered bio-sensing actuator. Sens. Actuators B: Chem. 196, 429–433.

Hou, L., Wu, X., Chen, G., Yang, H., Lu, M., Tang, D., 2015. HCR-stimulated formation of DNAzyme concatamers on gold nanoparticle for ultrasensitive impedimetric immunoassay. Biosens. Bioelectron. 68, 487–493.

Hou, L., Tang, Y., Xu, M., Gao, Z., Tang, D., 2014a. Tyramine-based enzymatic conjugate repeats for ultrasensitive immunoassay accompanying tyramine signal amplification with enzymatic biocatalytic precipitation. Anal. Chem. 86, 8352–8358.

Hou, L., Gao, Z., Xu, M., Cao, X., Wu, X., Chen, G., Tang, D., 2014b. DNAzyme-functionalized gold–palladium hybrid nanostructures for triple signal amplification of impedimetric immunosensor. Biosens. Bioelectron. 54, 365–371.

Hou, L., Cui, Y., Xu, M., Gao, Z., Huang, J., Tang, D., 2013. Graphene oxide-labeled sandwich-type impedimetric immunoassay with sensitive enhancement based on enzymatic 4-chloro-1-naphthol oxidation. Biosens. Bioelectron. 47, 149–156.

Inose, K., Fujikawa, M., Yamazaki, T., Kojima, K., Sode, K., 2003. Cloning and expression of the gene encoding catalytic subunit of thermostable glucose dehydrogenase from *Burkholderia cepacia* in *Escherichia coli*. Biochim. Biophys. Acta 1645, 133–138.

Ito, K., Okuda-Shimazaki, J., Mori, K., Kojima, K., Tsugawa, W., Ikebukuro, K., Lin, C., E., La Belle, J., Yoshida, H., Sode, K., 2019. Designer fungus FAD glucose dehydrogenase capable of direct electron transfer. Biosens. Bioelectron. 123, 114–123.

Kakehi, N., Yamazaki, T., Tsugawa, W., Sode, K., 2007. A novel wireless glucose sensor employing direct electron transfer principle based enzyme fuel cell. Biosens. Bioelectron. 22, 2250–2255.

Katz, E., Willner, I., 2003. Probing biomolecular interactions at conductive and semiconductive surfaces by impedance spectroscopy: routes to impedimetric immunosensors, DNA-sensors, and enzyme biosensors. Electroanalysis 15, 913–947.

Lee, I., Loew, N., Tsugawa, W., Ikebukuro, K., Sode, K., 2019. Development of a third-generation glucose sensor based on the open circuit potential for continuous glucose monitoring. Biosens. Bioelectron. 124–125, 216–223.

Lee, I., Loew, N., Tsugawa, W., Lin, C., E., Probst, D., LaBelle, J., T., Sode, K., 2018. The electrochemical behavior of a FAD dependent glucose dehydrogenase with direct electron transfer subunit by immobilization on self-assembled monolayers. Bioelectrochemistry 121, 1–6.

Lee, I., Sode, T., Loew, N., Tsugawa, W., Lowe, C.R., Sode, K., 2017. Continuous operation of an ultra-low-power microcontroller using glucose as the sole energy source. Biosens. Bioelectron. 93, 335–339.

Lisdat, F., Schäfer, D., 2008. The use of electrochemical impedance spectroscopy for biosensing. Anal. Bioanal. Chem. 391, 1555–1567.

Okuda, J., Sode, K., 2004. PQQ glucose dehydrogenase with novel electron transfer ability. Biochem. Biophys. Res. Commun. 394, 793–797.

Okuda, J., Yamazaki, T., Fukasawa, M., Kakehi, N., Sode, K., 2007. The application of engineered glucose dehydrogenase to a direct electron–transfer-type continuous glucose monitoring system and a compartmentless biofuel cell. Anal. Lett. 40, 431–440.

Okuda-Shimazaki, J., Kakehi, N., Yamazaki, T., Tomiyama, M., Sode, K., 2008. Biofuel cell system employing thermostable glucose dehydrogenase. Biotechnol. Lett. 30, 1753–1758.

Okuda-Shimazaki, J., Loew, N., Hirose, N., Kojima, K., Mori, K., Tsugawa, W., Sode, K., 2018. Construction and characterization of FAD glucose dehydrogenase complex harboring truncated electron transfer subunit. Electrochim. Acta 277, 276–286.

Prodromidis, M., I., 2010. Impedimetric immunosensors—a review. Electrochim. Acta 55, 4227–4233.

Ruecha, N., Shin, K., Chailapakul, O., Rodthongkum, N., 2019. Label-free paper-based electrochemical impedance immunosensor for human interferon gamma detection. Sens. Actuators B: Chem. 279, 298–304.

Sakai, G., Kojima, K., Mori, K., Oonishi, Y., Sode, K., 2015. Stabilization of fungi-derived

recombinant FAD-dependent glucose dehydrogenase by introducing a disulfide bond. Biotechnol. Lett. 37, 1091–1099.
Shervedani, R., K., Mehrjardi, A., H., Zamiri, N., 2006. A novel method for glucose determination based on electrochemical impedance spectroscopy using glucose oxidase self-assembled biosensor. Bioelectrochemistry 69, 201–208.
Shiota, M., Yamazaki, T., Yoshimatsu, K., Kojima, K., Tsugawa, W., Ferri, S., Sode, K., 2016. Bioelectrochemistry 112, 178–183.
Sode, K., Loew, N., Ohnishi, Y., Tsuruta, H., Mori, K., Kojima, K., Tsugawa, W., LaBelle, J., T., Klonoff, D., C., 2017. Novel fungal FAD glucose dehydrogenase derived from *Aspergillus niger* for glucose enzyme sensor strip. Biosens. Bioelectron. 87, 305–311.
Sode, K., Tsugawa, W., Yamazaki, T., Watanabe, M., Ogasawara, N., Tanaka, M., 1996. A novel thermostable glucose dehydrogenase varying temperature properties by altering its quaternary structures. Enzym. Microb. Technol. 19, 82–85.
Tsuya, T., Ferri, S., Fujikawa, M., Yamaoka, H., Sode, K., 2006. Cloning and functional expression of glucose dehydrogenase complex of *Burkholderia cepacia* in *Escherichia coli*. J. Biotechnol. 123, 127–136.
Vadim, F. Lvovich, 2012. Impedance Spectroscopy Applications to Electrochemical and Dielectric Phenomena. John Wiley & Sons, Inc, Hoboken.
Vidakovi´c-Koch, T., Mittal, V., K., Do, T., Q., N., Varni˘ ci´, M., Sundmacher, K., 2013. Application of electrochemical impedance spectroscopy for studying of enzyme kinetics. Electrochim. Acta 110, 94–104.
Wang, H., Ohnuki, H., Endo, H., Izumi, M., 2015. Impedimetric and amperometric bifunctional glucose biosensor based on hybrid organic-inorganic thin films. Bioelectrochemistry 101, 1–7.
Yamaoka, H., Ferri, S., Fujikawa, M., Sode, K., 2004. Essential role of the small subunit of thermostable glucose dehydrogenase from *Burkholderia cepacia*. Biotechnol. Lett. 26, 1757–1761.
Yamaoka, H., Sode, K., 2007. SPCE based glucose sensor employing novel thermostable glucose dehydrogenase, FADGDH: blood glucose measurement with 150nL sample in one second. J. Diabetes Sci. Technol. 1, 28–35.
Yamashita, Y., Ferri, S., Huynh, M., L., Shimizu, H., Yamaoka, H., Sode, K., 2013. Direct electron transfer type disposable sensor strip for glucose sensing employing an engineered FAD glucose dehydrogenase. Enzym. Microb. Technol. 52, 123–128.
Yamashita, Y., Suzuki, N., Hirose, N., Kojima, K., Tsugawa, W., Sode, K., 2018. Mutagenesis study of the cytochrome c subunit responsible for the direct electron transfer-type catalytic activity of FAD-dependent glucose dehydrogenase. Int. J. Mol. Sci. 19, 931.
Yamazaki, T., Tsugawa, W., Sode, K., 1999. Subunit analyses of a novel thermostable glucose dehydrogenase showing different temperature properties according to its quaternary structure. Appl. Biochem. Biotechnol. 77, 325–335.
Yamazaki, T., Okuda-Shimazaki, J., Sakata, C., Tsuya, T., Sode, K., 2008. Construction and characterization of direct electron transfer-type continuous glucose monitoring system employing thermostable glucose dehydrogenase complex. Anal. Lett. 41, 2363–2373.